Astronomy & Astrophysics manuscript no.
(will be inserted by hand later)

Flare Generated Acoustic Oscillations in Solar and Stellar Coronal Loops

D. Tsiklauri[1], V.M. Nakariakov[2], T.D. Arber[2], and M.J. Aschwanden[3]

[1] Joule Physics Laboratory, School of Computing, Science & Engineering, University of Salford, Salford, M5 4WT, England, UK
[2] Physics Department, University of Warwick, Coventry, CV4 7AL, England, UK
[3] Lockheed Martin, Advanced Technology Center Solar & Astrophysics Laboratory, Dept. L9-41, Bldg.252 3251 Hanover Street, Palo Alto, CA 94304, USA

Received ??? 2004 / Accepted ??? 2004

Abstract. Low-frequency longitudinal oscillations of a flaring coronal loop are studied numerically. In the recent work of Nakariakov et al. A&A, 414, L25-L28 (2004) it has been shown that the time dependences of density and velocity in a flaring loop contain well-pronounced quasi-harmonic oscillations associated with a 2nd harmonic of a standing slow magnetoacoustic wave. In this work we investigate physical nature of these oscillations in greater detail, namely, we study their spectrum (using periodogram technique) and how does heat positioning affects the mode excitation. We found that excitation of such oscillations practically independent of the positioning of the heat deposition in the loop. Because of the change of the background temperature and density, the phase shift between the density and velocity perturbations is not exactly equal to the quarter of the period, it varies along the loop and is time dependent, especially in the case of one footpoint (asymmetric) heating.

Key words. Sun: flares – Sun: oscillations – Sun: Corona – Stars: flare – Stars: oscillations – Stars: coronae

1. Introduction

Magnetohydrodynamic (MHD) coronal seismology is the main reason for studying waves in the solar corona. Also such studies are important in connection with coronal heating and solar wind acceleration problems. Observational evidence in the EUV coronal emission of coronal waves and oscillations is numerous (e.g. (Ofman et al. 1999, Ofman & Wang 2002)). Radio band observations also demonstrate various kinds of oscillations (e.g., the quasi-periodic pulsations, or QPP, see (Aschwanden 1987) for a review), usually with the periods from a few seconds to tens of seconds. Also, decimeter and microwave observations show much longer periodicities, often in association with a flare. For example, (Wang & Xie 2000) observed QPP with the periods of about 50 s at 1.42 and 2 GHz (in association with an M4.4 X-ray flare). Similar periodicities have been observed in the X-ray band (e.g., (McKenzie & Mullan 1997, Terekhov et al. 2002)) and in the white-light emission associated with the stellar flaring loops (Mathioudakis et al. 2003). A possible interpretation of these medium period QPPs may be interpreted in terms of kink or torsional modes (Zaitsev & Stepanov 1989). In our previous, preliminary study (Nakariakov et al. 2004), we have outlined an alternative, *simpler, thus more aesthetically attractive*, mechanism for generation of long-period QPPs. In this study we *demonstrate in detail,* that in a coronal loop an impulsive (time-transient) energy release efficiently generates the second spatial harmonics of a slow magnetoacoustic mode. In particular, in the present study we study the spectrum (using periodogram technique) of these oscillations and how does heat positioning affects the mode excitation.

Send offprint requests to: David Tsiklauri,
e-mail: D.Tsiklauri@salford.ac.uk

2. Numerical Results

The model that we use to describe plasma dynamics in a coronal loop is outlined in (Nakariakov et al. 2004). Here we just add that, when solving numerically 1D radiative hydrodynamic equations (infinite magnetic field approximation), and using a 1D version of Lagrangian Re-map code (Arber et al. 2001) with the radiative loss limiters,

the radiative loss function was specified as

$$L_r(T) = n_e^2 \begin{cases} 10^{-26.60}\, T^{1/2} & T > 10^{7.6} \\ 10^{-17.73}\, T^{-2/3} & 10^{6.3} < T < 10^{7.6} \\ 10^{-21.94} & 10^{5.8} < T < 10^{6.3} \\ 10^{-10.40}\, T^{-2} & 10^{5.4} < T < 10^{5.8} \\ 10^{-21.2} & 10^{4.9} < T < 10^{5.4} \\ 10^{-31}\, T^{2} & 10^{4.6} < T < 10^{4.9} \\ 10^{-21.85} & 10^{4.3} < T < 10^{4.6} \\ 10^{-48.31}\, T^{6.15} & 10^{3.9} < T < 10^{4.3} \\ 10^{-69.90}\, T^{11.7} & 10^{3.6} < T < 10^{3.9} \end{cases}$$

which is (Rosner et al. 1978) law extended to a wider temperature range (Peres et al. 1982, Priest 1982).

We have used the same heating function as in (Nakariakov et al. 2004). The choice of the temporal part of the heating function is such that at all times there is a small background heating present (either at footpoints or the loop apex) which ensures that in the absence of flare heating (when α, that determines flare heating amplitude, is zero) the average loop temperature stays at 1 MK. For easy comparison between that apex and footpoint heating cases, with fix, Q_p, flare heating amplitude at a given different value in each case (which ensures that with the flare heating on when $\alpha = 1$ the average loop temperature peaks at about the observed value of 30 MK in *both cases*).

In all our numerical runs, presented here, $1/(2\sigma_s^2)$ was fixed at 0.01 Mm^{-2}, which gives the heat deposition length scale, $\sigma_s = 7$ Mm. This is a typical value determined from the observations (Aschwanden et al. 2002). The flare peak time was fixed in our numerical simulations at 2200 s. The duration of flare, σ_t, was fixed at 333 s. The time step of data visualization (which in fact is much larger than the actual time step, 0.034 s, in the numerical code) was chosen to be 0.5 s.

2.1. Case of Apex (Symmetric) Heating

In this subsection we complete analysis started in (Nakariakov et al. 2004), namely for the same numerical run we study spectrum of the detected oscillations at different spatial points.

As it was pointed out in (Nakariakov et al. 2004), the most interesting fact is that we see clear quasi-periodic oscillations, especially in the second stage (peak of the flare) for time interval $t = 2500 - 2800$ s (cf. Fig. 1 in (Nakariakov et al. 2004)). In fact, such oscillations are frequently seen during the solar flares observed in X-rays, 8-20 keV, (e.g. Terekhov et al. (2002)) as well as stellar flares observed in white-light (e.g. Mathioudakis et al. (2003)).

Before we start discussion of the physical nature of these oscillations, first let us recall for completeness what simple 1D analytic theory of standing sound waves tells us: If we use 1D, linearized, hydrodynamic equations with constant unperturbed (zero order) background variables,

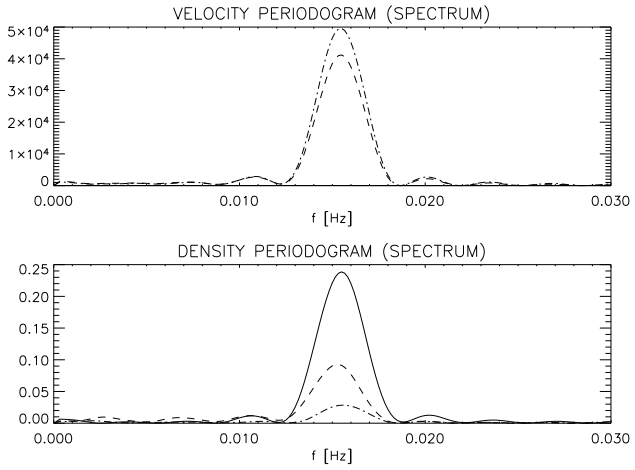

Fig. 1. Case of apex (symmetric) heating: Periodogram (spectrum) of the velocity and density oscillatory component times series outputted in the following three points: loop apex (solid curve), 1/4 (dash-dotted curve) and 1/6 (dashed curve) of the effective loop length (48 Mm), i.e. at $s = 0, -12, -16$ Mm.

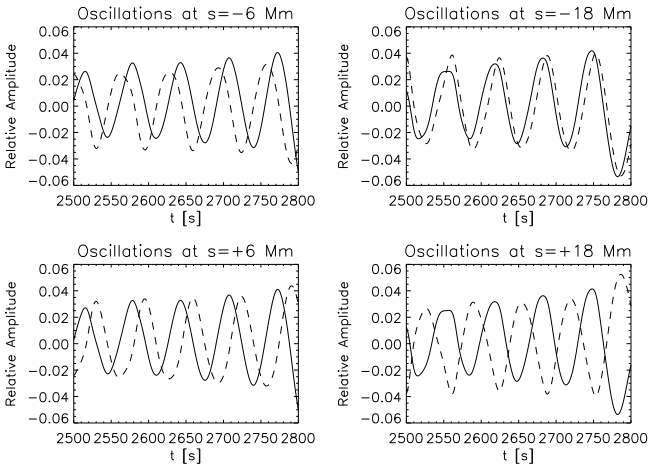

Fig. 2. Case of apex (symmetric) heating: oscillatory components of time series outputted at ±6 Mm and ±18 Mm in the time interval of 2500-2800 s. The solid curve shows plasma number density in units of 10^{11} cm^{-3}. The dashed curve shows velocity normalized to 400 km s^{-1}.

the solutions for density, ρ and velocity, V_x, can be easily written as

$$V_x(s,t) = A\cos\left(\frac{n\pi C_s}{L}t\right)\sin\left(\frac{n\pi}{L}s\right), \quad (1)$$

$$\rho(s,t) = -\frac{A\rho_0}{C_s}\sin\left(\frac{n\pi C_s}{L}t\right)\cos\left(\frac{n\pi}{L}s\right), \quad (2)$$

where C_s is a speed of sound, A is wave amplitude, L is loop length, $n = 1, 2, 3, ...$ is a number of harmonic, and s is a distance along the loop. Note that (relative) phase shift between V_x and ρ is $\Delta P/P = -(\pi/2)/(2\pi) = -1/4$, where P is standing wave period.

In Fig. 1 we present periodogram (spectrum) of the velocity and density oscillatory component times series outputted in the following three points: loop apex, 1/4 and 1/6 of the effective loop length (48 Mm), i.e. at $s = 0, -12, -16$ Mm. The choice first two points is obvious because we wanted to test whether simple analytic solution for 1D standing sound waves (see below) is at all relevant in this case. The third point (1/6) was chosen arbitrarily (any spatial point along the loop where density and velocity of the standing waves does not have a node would be equally acceptable). We gather from the graph that as expected for 2nd spatial harmonic of a standing sound wave in the velocity periodogram there are two clearly defined peaks and the largest peak corresponds to 1/4 of the effective loop length, while smaller peak corresponds to the 1/6. Note that at the loop apex periodogram gives 0 (solid line is too close to zero to be seen in the plot). While density periodogram is exactly opposite to the velocity one. Largest peak corresponds to the loop apex, while 1/6 of the effective loop length corresponds to a smaller peak, and 1/4 is quite small (close to zero). Location of the peaks are at about 0.0155 Hz i.e. period of the oscillation is 64 s. Period of a 2nd spatial harmonic of a standing sound wave should be

$$P = L/C_s = L/(1.52 \times 10^5 \sqrt{T}), \quad (3)$$

where T is plasma temperature measured in MK. If we substitute effective loop length $L = 48$ Mm (see Fig. 2 in (Nakariakov et al. 2004)) and an average temperature of 25 MK (see top panel in Fig. 1 in (Nakariakov et al. 2004) in the range of 2500-2800 s – quasi periodic oscillations time interval we study) we obtain 63 s, which is quite close to the result of our numerical simulation. In fact, such a close coincidence is surprising bearing in mind that the theory does not take into account variation of background density and velocity in time, while we see from Fig. 1 in (Nakariakov et al. 2004) that even within considered short interval during the flare 2500-2800 s all physical quantities vary in time significantly. To close our investigation of the physical nature of the oscillations, we study the phase shift between velocity and density oscillations, and compare our simulation results with the 1D analytic theory. In Fig. 2 we plot oscillatory components of time series outputted at ± 6 and ± 18 Mm of plasma number density in units of 10^{11} cm^{-3} and velocity, normalized to 400 km s^{-1} (note that sound speed at 25 MK is 760 km s^{-1} which roughly is within the $t = 2500 - 2800$ s). These points where selected so that one symmetric (with respect to the apex) pair (± 6 Mm) is close to the apex, while another pair (± 18 Mm) is closer to footpoints. We gather from this graph: (A) clear quasi periodic oscillations are present; (B) that they are shifted with respect to each other in time; (C) in the case of the pair close to the apex (± 6 Mm) the phase shift is quite close to the one predicted by the 1D analytic theory; (D) in the case of the pair close to the footpoints (± 18 Mm) the phase shift is somewhat different from the one predicted by the 1D analytic theory. In the latter case the discrepancy can be attributed to the presence flows close to the footpoints. Main reason for the overall deviation is due to fact that analytic theory does not take into account variation of background density and velocity in time, and the fact that density gradients in the transition region are not providing perfect reflecting boundary conditions for the formation of standing sound waves.

Yet another interesting result is that even with wide variation of the parameter space of the flare, its duration, peak average temperature, etc. we always obtained dominant 2nd spatial harmonic of a standing sound wave with some small admixture of 4th and sometimes 6th harmonic. Our initial guess was that this is due to the symmetric excitation of these oscillations (recall that we use apex heat deposition). In order to investigate this the issue of excitation further we decided to break symmetry and put heating source at one footpoint, hoping to see excitation of odd harmonics 1st, 3rd, etc.

2.2. Case of Single Footpoint (Asymmetric) Heating

In the case of single footpoint heating we fix $s_0 = 30$ Mm in Eq.(1) in (Nakariakov et al. 2004), i.e. (spatial) peak of the heating is chosen to be at the bottom of the transition region (top of chromosphere). Initially we run our numerical code without flare heating, i.e. we put $\alpha = 0$ (in this manner we turn off flare heating). $E_0 = 0.02$ erg cm^{-3} s^{-1}, was chosen such that in the steady (non-flaring) case the average loop temperature stays at about 1 MK. Then, we run our numerical code with flare heating, i.e. we put $\alpha = 1$, and fix Q_p at 1×10^4, so that it yields peak average temperature of about 30 MK. The results are presented in Fig. 3. We gather from the graph that during the flare apex temperature peaks at 38.38 MK while the number density at the apex at 3.11×10^{11} cm^{-3}. In this case, as opposed to the case of symmetric (apex) heating, velocity dynamics is quite different. Namely, since the symmetry of heating is broken, there is non zero net flow through the apex at all times. However, as in the symmetric heating case, we again see quasi-periodic oscillations superimposed on the dynamics of all physical quantities (cf time interval of $t = 2400 - 2700$ in Fig. 3). In what follows we do analysis of their physical nature as in the previous subsection.

In Fig. 4 we present time-distance plots of velocity and density in the time interval 2400-2700s, where the quasi-periodic oscillations are most clearly seen. Here we again subtracted the slow varying with respect to oscillation period background. The picture is quite different from the case of apex (symmetric) heating (compare it with Fig. 2 in (Nakariakov et al. 2004)). It is looks more complex because in this case the node in the velocity (at the apex) moves back and forth periodically along the apex, and for larger times ($t > 2550$ s) stronger flows (darker bands with at a slope) are now present. However, physical nature of the oscillations remains mainly the same – 2nd spatial harmonic of a sound wave (though with oscillating node along the apex).

To investigate this further we plot in Fig. 5 periodogram (spectrum) of the velocity and density oscillatory component times series outputted in the following three points: loop apex, 1/6 and 1/4 of the effective loop length. We gather from the graph that the periodogram (spectrum) is more complex than in the case of apex (symmetric) heating. Namely, in the velocity periodogram at the apex we see a peak with frequency of the oscillation different (higher) than that of 2nd spatial harmonic of a standing sound wave. Actually that is the frequency with which node of the velocity oscillates (see discussion in the previous paragraph). It has nothing to do with the standing mode, and it is rather dictated by the excitation conditions in the dynamics resonator, which the considered loop obviously is. Let us analyze now how this periodogram compares with the 1D analytic theory. Peak in the periodogram corresponding to 1/6 of the effective loop length (dashed line) corresponds to frequency of about 0.017 Hz, i.e. period of the oscillation is 59 s. Again, the period of a 2nd spatial harmonic of a standing sound wave should be calculated from Eq. (3). If we substitute effective loop length $L = 48$ Mm (see Fig. 4) and an average temperature of 26 MK (see top panel in Fig. 3 in the range of 2400-2700 s – quasi periodic oscillations time interval we study) we obtain 62 s, which is quite close to the result of our numerical simulation (59 s).

Next, we study the phase shift between velocity and density oscillations, and compare our simulation results with the 1D analytic theory. In Fig. 6 we produce a plot similar to Fig. 2, but for the case of asymmetric heating. The deviation which is greater than in the case apex (symmetric) heating can again be attributed to the oversimplification of the 1D analytic theory, which does not take into account time variation of the background physical quantities and imperfection of the reflecting boundary conditions (see above). And, more importantly, in the asymmetric case strong flows are present throughout of the flare simulation time, thus, if, say, linear time dependence would be assumed, which is relatively good within considered short interval during the flare 2400-2700 s, the Eqs(1)-(2) would be modified such that phase shift would vary secularly in time, which is similar to what we see in Fig. 6.

Yet another interesting observation comes from the following argument: in a steady 1D case analytic theory predicts that the phase shift between the density and velocity should be (A) zero for for a *propagating* acoustic wave and (B) quarter of a period for the *standing* acoustic wave. Since in the asymmetric case strong flows are present, we see less phase shift between the velocity and density in Fig. 6 as one would expect.

Thus, the results of the present study provide further *more definitive* than in (Nakariakov et al. 2004) proof that these oscillations indeed are 2nd spatial harmonic of a standing sound wave. However, present work also revealed that in the case of single footpoint (asymmetric) heating the physical nature of the oscillations is more complex as

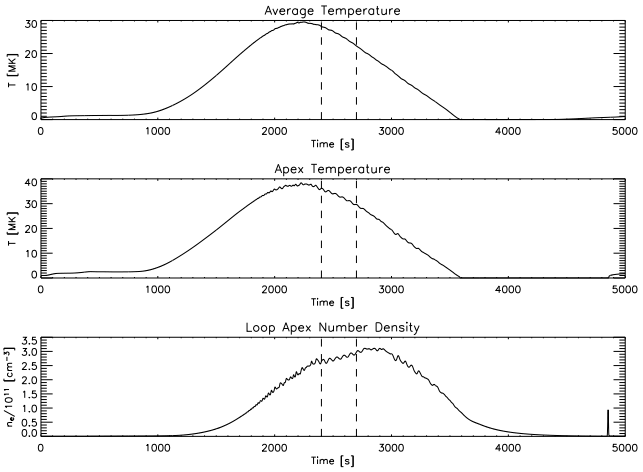

Fig. 3. Case of single footpoint (asymmetric) heating: Average temperature, temperature at apex, and number density at apex as a function of time.

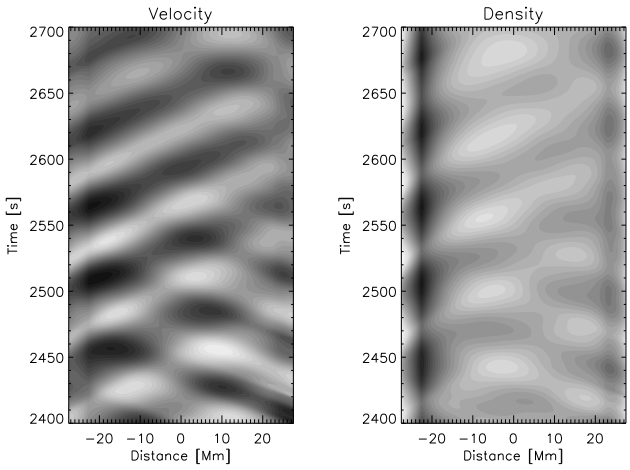

Fig. 4. Time-distance plots of the velocity and density oscillatory components in the time interval of 2400-2700s for the case of single footpoint (asymmetric) heating.

the node in the velocity oscillates along the apex and net flows are present.

3. Conclusions

Initially we have used 1D radiative hydrodynamics loop model which incorporates the effects of gravitational stratification, heat conduction, radiative losses, added external heat input, presence of Helium, hydrodynamic non-linearity, and bulk Braginskii viscosity to simulate flares (Tsiklauri et al. 2004). As a byproduct of that study, in practically all our numerical runs we have detected quasi periodic oscillations in all physical quantities (Nakariakov et al. 2004). In fact, such oscillations are frequently seen during the solar flares observed in X-rays, 8-20 keV (e.g. Terekhov et al. (2002)) as well as stellar flares observed in white-light (e.g. Mathioudakis et al. (2003)). Our present analysis shows, *in detail*, that quasi

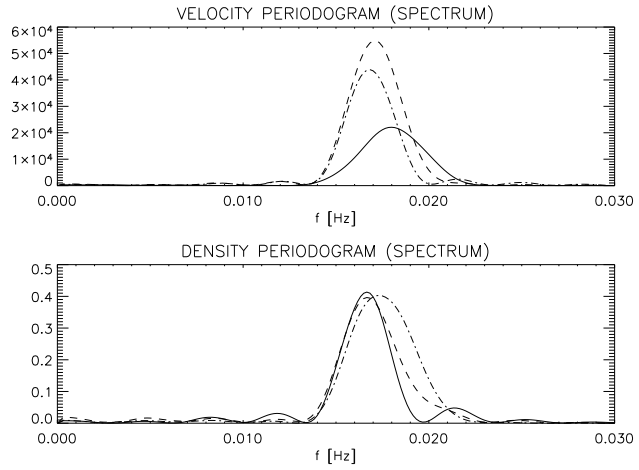

Fig. 5. As is Fig. 1 but for the case of single footpoint (asymmetric) heating. Time interval here is 2400-2700s.

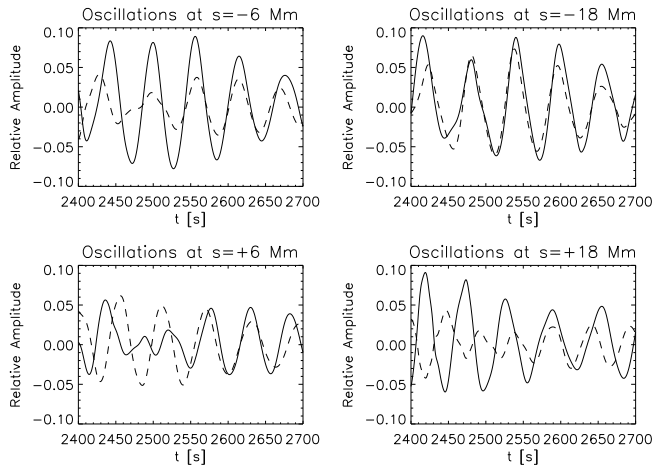

Fig. 6. As in Fig. 2, but for the case of single footpoint (asymmetric) heating. Time interval here is 2400-2700s.

periodic oscillations seen in our numerical simulations bear many similar features as the observed ones. In summary (Nakariakov et al. 2004) and the present study established the following features:

- We show that the time dependences of density and temperature in a flaring loop contain well-pronounced quasi-harmonic oscillations associated with standing slow magnetoacoustic modes of the loop.
- For *a wide range of physical parameters*, the dominant mode is the second spatial harmonic, with a velocity oscillation node and the density oscillation maximum at the loop apex. *This result is practically independent of the positioning of the heat deposition in the loop.*
- Because of the change of the background temperature and density, and the fact that density gradients in the transition region are not providing perfect reflecting boundary conditions for the formation of standing sound waves, the phase shift between the density and velocity perturbations is not exactly equal to the quarter of the period.
- We conclude that the oscillations in the white light, the radio and X-ray light curves observed during solar and stellar flares may be produced by the slow standing mode, with the period determined by the loop temperature and length.
- For a typical solar flaring loop the period of oscillations is shown to be about a few minutes, while amplitudes are typically few percent.

The novelties brought about by this study are that by studying the spectrum and phase shift of these oscillations we provide more definite proof that these oscillations are indeed 2nd harmonic of a standing sound wave, and that the single footpoint (asymmetric) heat positioning still produces 2nd spatial harmonic, though it is more complex than the apex (symmetric) heating (due to the presence of flows).

Acknowledgements. This research was supported in part by PPARC, UK. Numerical calculations of this work were performed using the PPARC funded Compaq MHD Cluster at St Andrews and Astro-Sun cluster at Warwick.

References

Arber, T. D., Longbottom, A. W., Gerrard, C. L., Milne, A. M. 2001, J. Comput. Phys., 171, 151

Aschwanden, M.J. 1987 Sol. Phys. 111, 113,

Aschwanden, M. J., Alexander, D. 2001, Sol. Phys. 204, 93

Aschwanden M. J., Brown, J. C., & Kontar E. P. 2002, Sol. Phys. 210, 383

Mathioudakis, M., Seiradakis, J. H., Williams, D. R., Agvoloupis, S., Bloomfield, D. S., McAteer, R. T. J. 2003, A&A, 403, 1101

McKenzie, D.E., Mullan, D.J., Sol. Phys. 1997, 176, 127

Nakariakov, V.M., Tsiklauri, D., Kelly, A., Arber, T.D., Aschwanden, M.J. 2004, A&A, 414, L25-L28

Ofman L., Nakariakov V.M., DeForest C.E. 1999, ApJ 514, 441

Ofman L., Wang T.J. 2002, ApJ, 580, L85

Peres, G., Rosner, R., Serio, S., & Vaiana, G.S. 1982, ApJ, 252, 791

Priest, E. R. 1982, Solar Magnetohydrodynamics, D. Reidel Publ. Comp., Dordrecht, Holland

Rosner, R., Tucker, W. H., Vaiana, G. S. 1978, ApJ, 220, 643

Terekhov, O. V., Shevchenko, A. V., Kuz'min, A. G., Sazonov, S. Y., Sunyaev, R. A., Lund, N. 2002, Astron. Lett., 28, 397

Tsiklauri D. , M.J. Aschwanden, V.M. Nakariakov, and T.D. Arber 2004 (submitted for publication)

Wang, T., Solanki, S. K., Curdt, W., Innes, D. E., Dammasch, I. E. 2002, ApJ, 574, L101

Wang, M., Xie, R.X. 2000, Chin. Astron. Astrophys. 24, 95

Zaitsev, V.V., Stepanov, A.V. 1989, Sov. Astron. Lett. 15, 66